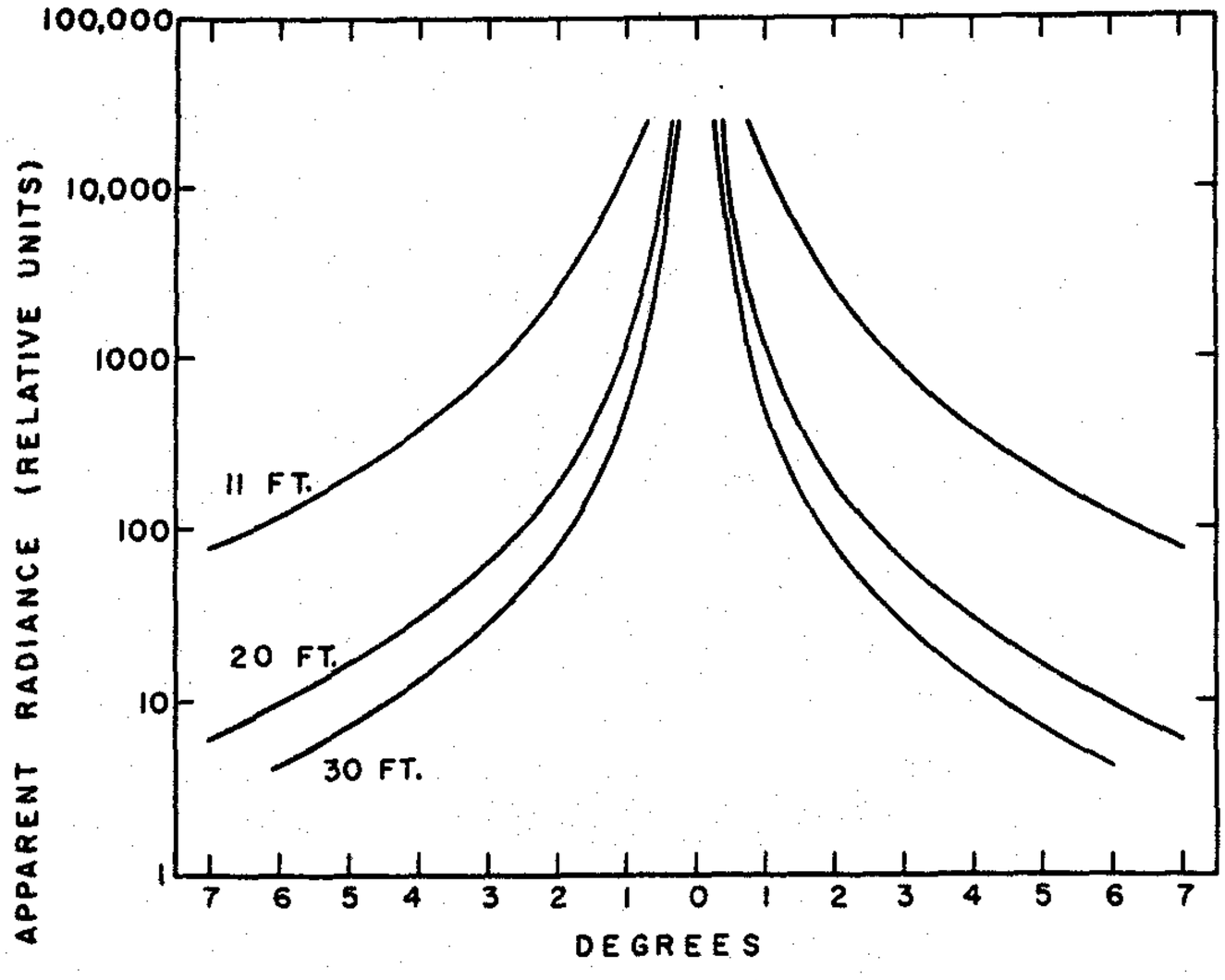


FIG. 1.66 Apparent radiance produced by beam of highly collimated flux (cf. Fig. 1.62), as found by Duntley, Lake Winnipesaukee, N.H., 11 August 1961. (Fig. 17 from [78], by permission)

(= 4.80 ft.) as measured via a Wratten No. 61 green filter, in Lake Winnipesaukee, N.H., summer, 1961. The locations of the measurements within the induced light field are indicated by the inset of the figure. The irradiated plane was swept by the moving beam.

Finally, Fig. 1.66 depicts the apparent radiance as observed under somewhat the same general test condition of Fig. 1.65. Now the beam had a $2\psi$ of 0.01° and was directed toward the telephotometer so that it completely filled the entrance pupil of the latter at all times. The water was slightly clearer in the present case, having an attenuation length of 2.04 meters (= 6.70 ft.), i.e., an $\alpha$ of .490/m (= .149/ft.) for the same wavelength band. It is of interest to compare Figs. 1.61 and 1.66, which reveal subtle differences between the radiance distributions found by looking at distant point sources and down the barrel of a collimated beam.

Some further discussion of these empirical findings, especially their applicability to underwater communications by scattered light, may be found in [79].

## 1.6 Inherent and Apparent Optical Properties of Hydrosols

The three simple models describing light fields in the seas and lakes of the earth, as developed in Sec. 1.3, may now be considered as reasonably established descriptions of radiative transfer in natural hydrosols. For as we have seen in our brief survey of their applications in Sec. 1.4 and 1.5, they can be used both to organize our accumulated empirical knowledge of natural light fields by means of faithful symbolic representations of our observations, and also to encourage, via simple mathematical manipulations, the exploration of

new and deeper physical phenomena connected with light fields in the sea. Implicit in the structure of these models are the optical properties we introduced during their construction, such as $\alpha$, $\sigma$, s, a, and $\kappa$.

Now, if the theoretical equations of hydrologic optics may be viewed as the *bones* of the subject, then certainly the optical properties $\alpha$, $\sigma$, $\kappa$ and the various related properties are the *meat* of the subject. Indeed, the equations provide the essential form of our discipline; but the numerical values of their parameters provide it with useful substance. It is our purpose in this section to sort out the principal optical properties used in hydrologic optics and to indicate their representative magnitudes. It is not our purpose at this time, however, to optically catalog the seas and lakes of the world; such a task still awaits a definitive effort, and lies outside the province of a work devoted to the theoretical principles of the subject.

## Operational Definitions of the Inherent Optical Properties

The fundamental inherent optical properties of hydrologic optics are the *volume attenuation function* $\alpha$, and the *volume scattering function* $\sigma$. They are *inherent* in the sense that their magnitudes for each wavelength depend only on the substances comprising the hydrosol and not on the geometric structure of the various light fields that may pervade it. The properties $\alpha$, and $\sigma$ are *fundamental* in the sense that the entire theory of hydrologic optics (and indeed radiative transfer theory) can be constructed from them, given the concept of the radiance function and the equation of transfer. The greatest contributions an experimental scientist can make to hydrologic optics at this stage of its development (or to any other branch of radiative transfer) lie in the detailed study --on physical, chemical, and optical levels--of these two fundamental properties, along with the simultaneous documentation of the light fields in optical media.* Chapter 13 is devoted to a detailed exposition of the operational definitions of these and other properties. Our immediate aim is to introduce these concepts with a minimum of preamble, though a full and deep understanding of them can come only after the contents of at least Chapters 2, 3, 8, 9 and 13 are mastered.

### The Volume Attenuation Function

The volume attenuation function $\alpha$ provides a measure of the loss of radiant flux from a beam of photons of a given wavelength induced by: (a) scattering of flux out of the direction of the beam without change in wavelength or: (b) by scattering of flux of the beam with a change of wavelength, or: (c) by outright absorption of some of the radiant energy

---

*Important problems concerning the physical makeup of $\alpha$ and $\sigma$ also await interested theoreticians. See problem III of Chapter XVI, Ref. [251].

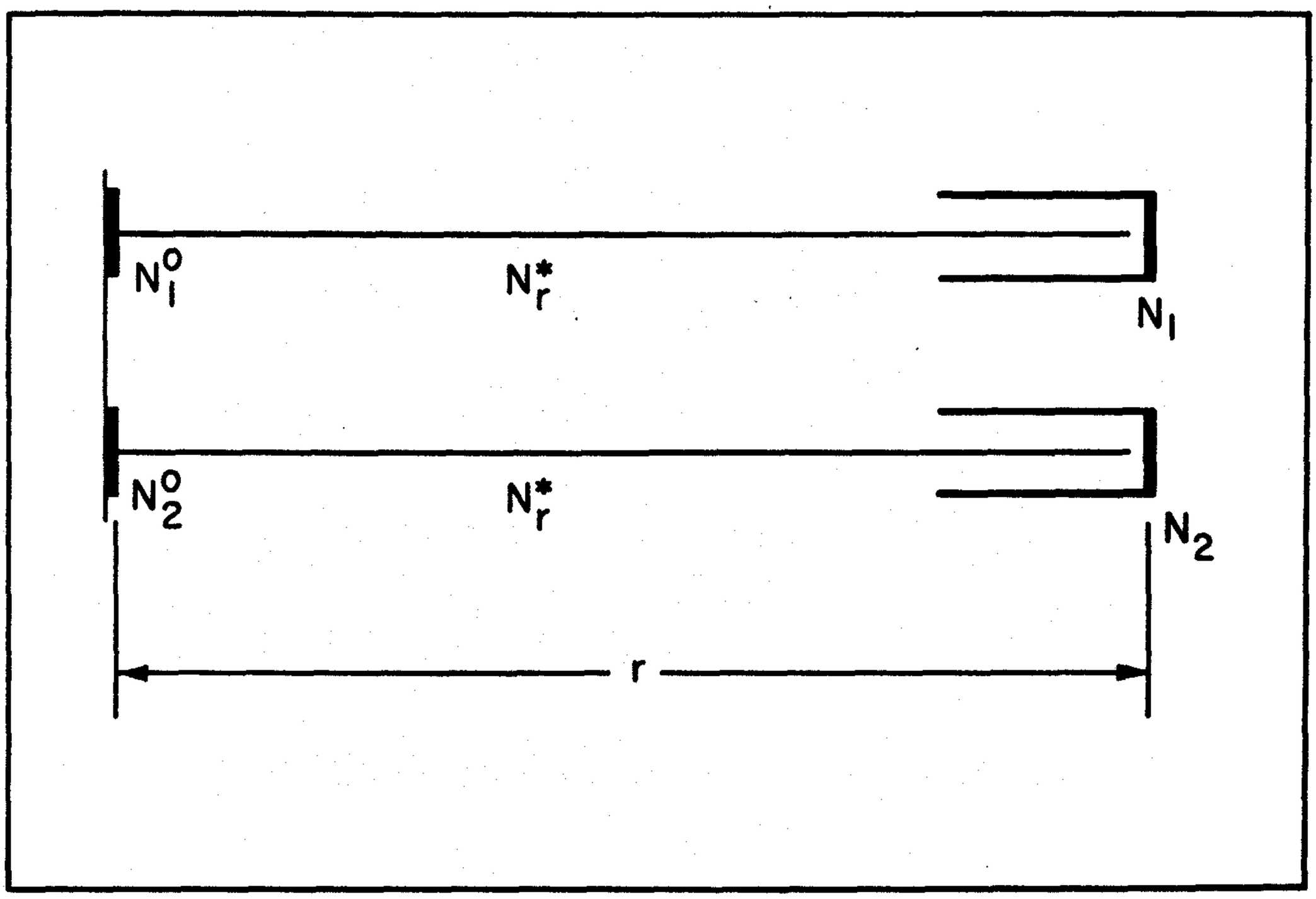


FIG. 1.67 Arrangement for an operational definition of volume attenuation function.

into a form of non-radiant energy. A particularly effective method of defining $\alpha$ is by means of the beam transmittance function using the fact that radiance differences of simultaneous beams propagate precisely in an exponential manner along close parallel paths.

Figure 1.67 depicts two parallel closely spaced paths of length r in an optical medium. The initial radiances at the beginning of the paths are $N_1^o$ and $N_2^o$, and matters are arranged so that the medium is homogeneous in the vicinity of the paths and that the path radiances of the two paths are essentially the same, and of common value $N^*$. If $T_r$ is the common fraction of photons comprising $N_1^o$ and $N_2^o$ transmitted along each path without having been scattered or absorbed, then by (24) of Sec. 1.3 the apparent radiances:

$$N_1 = N_1^o T_r + N^*$$

and

$$N_2 = N_2^o T_r + N^*$$

measured at the end of the path may be used to find the *beam transmittance* $T_r$ by means of the relation:

$$T_r = \frac{N_2 - N_1}{N_2^o - N_1^o} \tag{1}$$

It is very easy to see, using (1), that if two paths of

arbitrary lengths r and s are placed end to end to form a new straight path of length r+s, then:

$$0 \leq T_r \leq 1 \tag{2}$$

and:

$$T_{r+s} = T_r T_s \tag{3}$$

and also:

$$T_o = 1 \tag{4}$$

The second property is the *multiplicative* (or semigroup) property of beam transmittance. It is the basis of the exponential representation of $T_r$. Indeed, let us write:

$$\text{"}\alpha_r\text{"} \quad \text{for} \quad \frac{1-T_r}{r} \tag{5}$$

The quantity $\alpha_r$ is the (*empirical*) *volume attenuation function* because it gives the average amount of loss of radiance of a beam per unit length of travel of a beam of unit radiance. To see this let $N^o$ be an initial radiance starting out along a path of length r. Then $N^o T_r = N_r^o$ is the *residual radiance*, i.e., the radiance left over in the beam after scattering and absorption losses over the path. Hence $N^o - N_r^o$ is the actual radiance lost, and $(N^o - N_r^o)/r$ the average loss per unit length of the path. Dividing by $N^o$, we arrive at (5).

Now consider a path of length r+s. Then by (3) and (5):

$$\frac{T_{s+r} - T_r}{s} = \frac{T_s - 1}{s} T_r = -\alpha_s T_r$$

Using the definition of derivative applied to $T_r$, and letting $s \to 0$, we have:

$$\frac{dT_r}{dr} = -\alpha T_r \tag{6}$$

where we have written:

$$\text{"}\alpha\text{"} \quad \text{for} \quad \lim_{r \to 0} \alpha_r \tag{7}$$

From (4) and (6):

$$T_r = e^{-\alpha r} \tag{8}$$

for homogeneous media. This is the basic connection between beam transmittance and the *volume attenuation function* $\alpha$ defined in (7). The function $\alpha$ has dimensions of $L^{-1}$, and therefore units of $(\text{meter})^{-1}$. Observe that by (2), $\alpha_r$ and hence $\alpha$ is a non-negative quantity. From (8) we have:

$$\alpha = -\frac{1}{r} \ln T_r \tag{9}$$

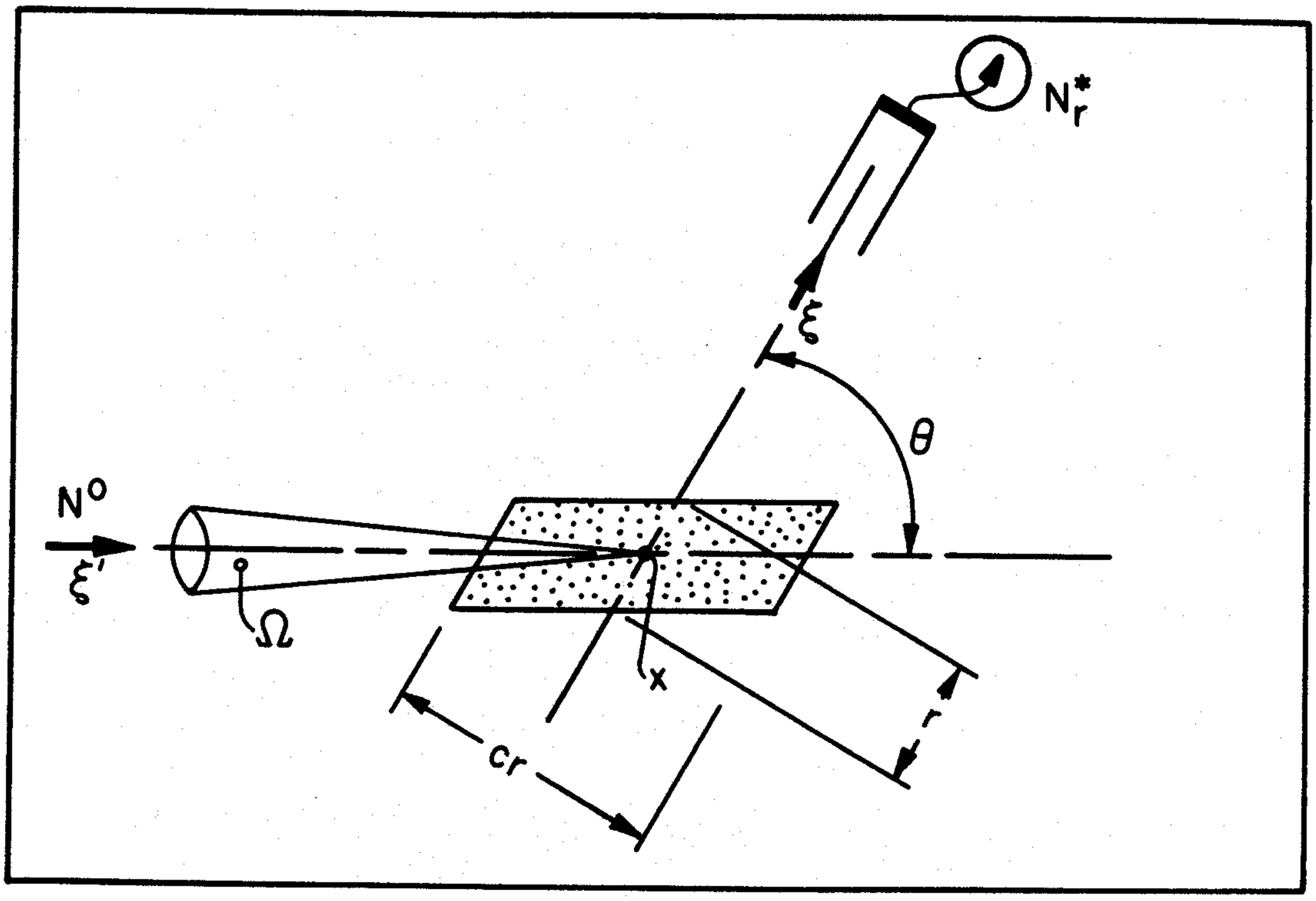


FIG. 1.68 Arrangement for an operational definition of volume scattering function.

which together with (1) provides a useful operational definition of $\alpha$. For a further discussion of these ideas see Secs. 13.2, 13.4 and 13.5.

## The Volume Scattering Function

A small volume of an optical medium is irradiated through a small set of directions of solid angle $\Omega$ about a direction $\xi'$ by a radiance $N^o$ of a given wavelength, and the scattered radiant flux in the direction $\xi$, at an angle $\theta$ with $\xi'$, is observed to be $N_r^*$, where r is the length of the line of sight through the volume. The volume is in the form of a parellelepiped whose dimensions are $r \times r \times cr$, where c is a constant. Then we write Errata

$$\text{"}\sigma_{r,\Omega}(\theta)\text{"} \quad \text{for} \quad \frac{N_r^*}{N^o r\Omega} \tag{10}$$

Further, we write:

$$\text{"}\sigma(\theta)\text{"} \quad \text{for} \quad \lim_{\substack{r\to 0 \\ \Omega\to 0}} \sigma_{r,\Omega}(\theta) \tag{11}$$

and call $\sigma$ the *volume scattering function*. A more detailed discussion of $\sigma$ is given in Sec. 13.6, and in Sec. 18 of Ref. [251]. The dimensions of $\sigma$ are $L^{-1}(sr)^{-1}$ and hence its units

are $(\text{meter})^{-1}(\text{steradian})^{-1}$.

The reason for choosing (11) as the basic definition of $\sigma(\theta)$ is that it yields at once the relation:

$$N_* = \frac{N_r^*}{r} = N^o\sigma(\theta)\Omega$$

which with care can be made to blossom into:

$$N_*(x,\xi) = \int_\Xi N(x,\xi')\sigma(x;\xi';\xi)\ d\Omega(\xi')$$

and which in turn is the standard representation of the path function in general radiative transfer theory. The correct logical order of appearance of $N_*$ and $\sigma$ in the theoretical construction of radiative transfer theory is given in the systematic discussions of Chapter 3.

An alternate form of $\sigma_{r,\Omega}(\theta)$ is given by writing

$$\text{"}\sigma_V(\theta)\text{"} \quad \text{for} \quad \frac{J_r^*}{H^oV} \tag{12}$$

where $H^o = N^o\Omega$, V is the volume (e.g., in this case $cr^3$) of the scattering region in Fig. 1.68, and $J_r^*$ is the radiant intensity of the scattered flux. Clearly

$$\sigma_V(\theta) = \sigma_{r,\Omega}(\theta) \tag{13}$$

and so the two definitions are equivalent. (A careful proof of this is given in Sec. 18 of Ref. [251].) It is found that $\sigma$ depends, in virtually any given practical setting, only on the angle $\theta$ between the incident direction $\xi'$ and the scattered direction $\xi$. Hence it is possible in practice to write "$\sigma(x;\xi';\xi)$" in the more compact way "$\sigma(\theta)$", adopted above.

## Volume Total Scattering Function and Volume Absorption Function

If $\sigma(\theta)$ is integrated over all $\theta$, we obtain the *volume total scattering function* s; where we write:

$$\text{"s"} \quad \text{for} \quad \int_{\phi=0}^{2\pi}\int_{\theta=0}^{\pi} \sigma(\theta)\ \sin\ \theta\ d\theta\ d\phi \tag{14}$$

The angle $\phi$ is measured around the direction $\xi'$ (in Fig. 1.68) as a hinge. Clearly we have:

$$s = 2\pi \int_{\theta=0}^{\pi} \sigma(\theta)\ \sin\ \theta\ d\theta \tag{15}$$

By splitting up the domain of integration $[0,\pi]$ into $[0,\pi/2]$ and $[\pi/2,\pi]$ and writing*:

$$\text{"f"} \quad \text{for} \quad 2\pi\int_{\theta=0}^{\pi/2} \sigma(\theta)\,\sin\theta\,d\theta \tag{16}$$

and

$$\text{"b"} \quad \text{for} \quad 2\pi\int_{\pi/2}^{\pi} \sigma(\theta)\,\sin\theta\,d\theta \tag{17}$$

We then have:

$$s = f + b \tag{18}$$

where f and b are the (volume) *forward* and *backward scattering functions* for collimated radiant flux.

The *volume absorption function* a comes in the back door of the theory by writing

$$\text{"a"} \quad \text{for} \quad \alpha\text{-}s\ , \tag{19}$$

but it redeems itself by possessing the following remarkably powerful operational form:

$$a = \frac{1}{h(z)}\,\frac{d\bar{H}(z,+)}{dz}\ , \tag{20}$$

discussed in the closing paragraph of Sec. 1.4 (see in particular (90) of Sec. 1.4, and also Sec. 13.8).

*Considered together, the three operational formulations of* $\alpha$, $\sigma$, *and* a *in (9), (10) and (20), respectively, form a complete, mutually consistent, independent set of experimental means of determining these inherent optical properties of natural or artificial hydrosols.* An ideal scientific study of a given hydrosol would determine $\alpha$,$\sigma$ and a using these independent means, and then check consistency by requiring the three sets of data to satisfy the relation:

$$\boxed{2\pi\int_{0}^{\pi} \sigma(\theta)\,\sin\theta\,d\theta = \alpha\text{-}a} \tag{21}$$

In other words, the measured $\sigma$ values are first integrated to yield the left side of (21). Then the measured a is subtracted from the independently measured $\alpha$, and, hopefully, this difference is equal within a reasonable error allowance, to the computed $\sigma$-integral, for each wavelength from the infrared to the ultraviolet parts of the electromagnetic spectrum, and for each point in a hydrosol at which the

---

*The general definitions are given in (1), (2) of Sec. 9.6.

three determinations were made. This check is expected to hold, in principle, for all unpolarized light fields (Sec. 13.11).

## Selected Physical Measurements of the Inherent Optical Properties

The following three tables provide representative samples of the inherent optical properties $\alpha$, $\sigma$, s, f, b and a, measured for distilled water, ocean water, and lake water. The measurements were made by Tyler [300] and may serve as an example of the careful and consistent types of measurements that may be used to optically document the natural waters of the world. Such types of measurements, when performed for a sufficiently finely spaced set of wavelengths, will begin to move hydrologic optics into its final stage of development as a mature scientific discipline.

In Table 1 the distilled water was of the commercially available kind, and is not "distilled" in the strictest sense of the word. The two samples do, however, provide a reasonably good basis for comparison with the $\sigma$'s of natural hydrosols. The wavelength band for the measurements was centered at 522 ± 80 mμ. The results compare favorably with those of Hulburt [115]. The Table 2 measurements were made in January 1961 in the four numbered locations shown in Fig. 1.69, and over the same wavelength band used for Table 1. Table 3

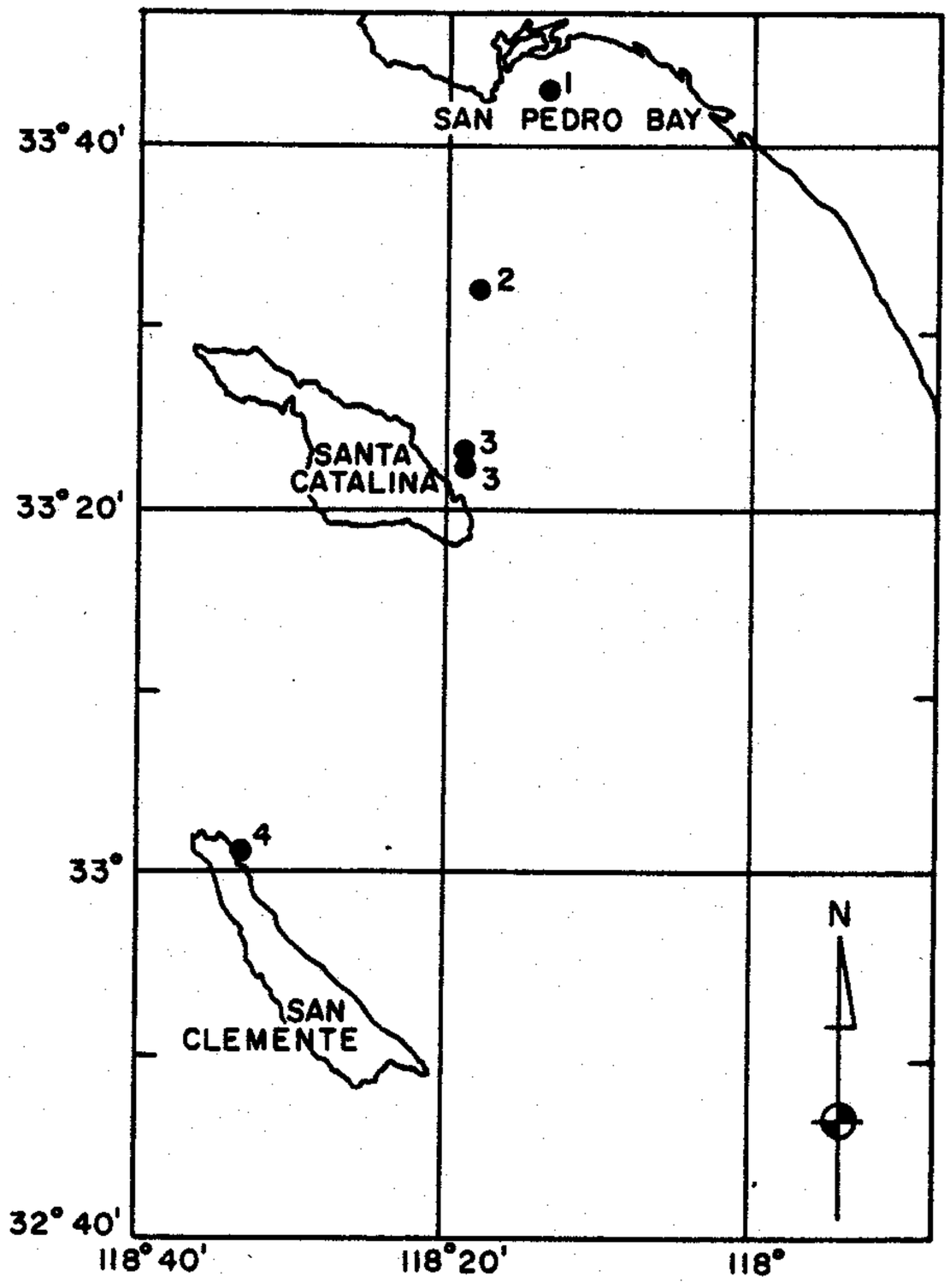


FIG. 1.69 Locations of Tyler's measurements off Southern California coast, winter 1960-1961, and as recorded in Table 2. (Fig. 1 from [300], by permission)

TABLE 1

Errata

Scattering properties of commercial "distilled" water samples. Bandwidth limited by a Wratten No. 57 filter.

| Sample | A | B |
|---|---|---|
| Volume attenuation coefficient $\alpha$/m | .062 | .047 |
| Volume total scattering coefficient s/m | .00845 | .00457 |
| Volume absorption coefficient a/m | .0536 | .0424 |
| Forward scattering coefficient f/m | .00763 | .00396 |
| Backward scattering coefficient f/m | .00082 | .000620 |
| Ratio f/s | .900 | .870 |
| Volume scattering function $\sigma(\theta)$ | | |
| $\theta$ = 0° | | |
| 10 | | |
| 20 | .00648 | .00316 |
| 30 | .00223 | .00107 |
| 40 | .000941 | .000520 |
| 50 | .000473 | .000294 |
| 60 | .000271 | .000191 |
| 70 | .000181 | .000128 |
| 80 | .000140 | .000096 |
| 90 | .000117 | .000083 |
| 100 | .000110 | .000079 |
| 110 | .000118 | .000082 |
| 120 | .000126 | .000092 |
| 130 | .000134 | .000102 |
| 140 | .000139 | .000112 |
| 150 | .000146 | .000119 |
| 160 | .000171 | .000141 |
| 170 | .000193 | .000161 |
| 180 | .000201 | .000169 |

(From [300], by permission)

TABLE 2

Scattering properties of Pacific Coastal and offshore water at the Stations shown in Figure 1.69. Bandwidth limited by a Wratten No. 57 filter.

| Station number | 1 | 2 | 3 | 4 |
|---|---|---|---|---|
| Volume attenuation coefficient α/m | .736 | .129 | .118 | .111 |
| Volume total scattering coefficient s/m | .125 | .01094 | .01420 | .0120 |
| Volume absorption coefficient a/m | .611 | .1181 | .1038 | .099 |
| Forward scattering coefficient f/m | .119 | .01010 | .01321 | .0110 |
| Backward scattering coefficient b/m | .00630 | .000847 | .000982 | .000984 |
| Ratio f/s | .950 | .925 | .930 | .915 |
| Volume scattering function σ(θ) | | | | |
| θ = 0° | | | | |
| 10 | | | | |
| 20 | .1014 | .00881 | .01192 | .00959 |
| 30 | .0360 | .00268 | .00358 | .00313 |
| 40 | .0152 | .00117 | .00145 | .00129 |
| 50 | .00739 | .000616 | .000698 | .000661 |
| 60 | .00419 | .000356 | .000396 | .000388 |
| 70 | .00266 | .000232 | .000253 | .000249 |
| 80 | .00181 | .000164 | .000179 | .000175 |
| 90 | .00134 | .000132 | .000145 | .000142 |
| 100 | .00109 | .000120 | .000134 | .000130 |
| 110 | .000940 | .000120 | .000135 | .000135 |
| 120 | .000903 | .000124 | .000146 | .000146 |
| 130 | .000912 | .000134 | .000158 | .000159 |
| 140 | .000944 | .000145 | .000175 | .000176 |
| 150 | .001003 | .000156 | .000192 | .000193 |
| 160 | .001028 | .000175 | .000202 | .000208 |
| 170 | .001036 | .000191 | .000206 | .000219 |
| 180 | .001037 | .000197 | .000207 | .000223 |

(From [300], by permission)

TABLE 3

Errata

Volume scattering function for Lake Pend Oreille, Idaho, Spring 1960 before and after a high wind. Bandwidth limited by a Wratten No. 45 filter.

| Sample date | | April 26 | April 27 |
|---|---|---|---|
| Volume attenuation coefficient α/m | | .589 | .909 |
| Volume total scattering coefficient s/m | | .258 | .585 |
| Volume absorption coefficient a/m | | .331 | .324 |
| Forward scattering function f/m | | .248 | .559 |
| Backward scattering coefficient b/m | | .00976 | .0256 |
| Ratio f/s | | .960 | .955 |
| Volume scattering function σ(θ) | | | |
| | θ = 0° | | |
| | 10 | | |
| | 20 | .222 | .470 |
| | 30 | .0715 | .166 |
| | 40 | .0291 | .0758 |
| | 50 | .0137 | .0380 |
| | 60 | .00712 | .0206 |
| | 70 | .00416 | .0121 |
| | 80 | .00271 | .00780 |
| | 90 | .00198 | .00559 |
| | 100 | .00162 | .00448 |
| | 110 | .00147 | .00394 |
| | 120 | .00143 | .00379 |
| | 130 | .00145 | .00372 |
| | 140 | .00149 | .00371 |
| | 150 | .00156 | .00383 |
| | 160 | .00163 | .00396 |
| | 170 | .00168 | .00406 |
| | 180 | .00170 | .00410 |

(From [300], by permission)

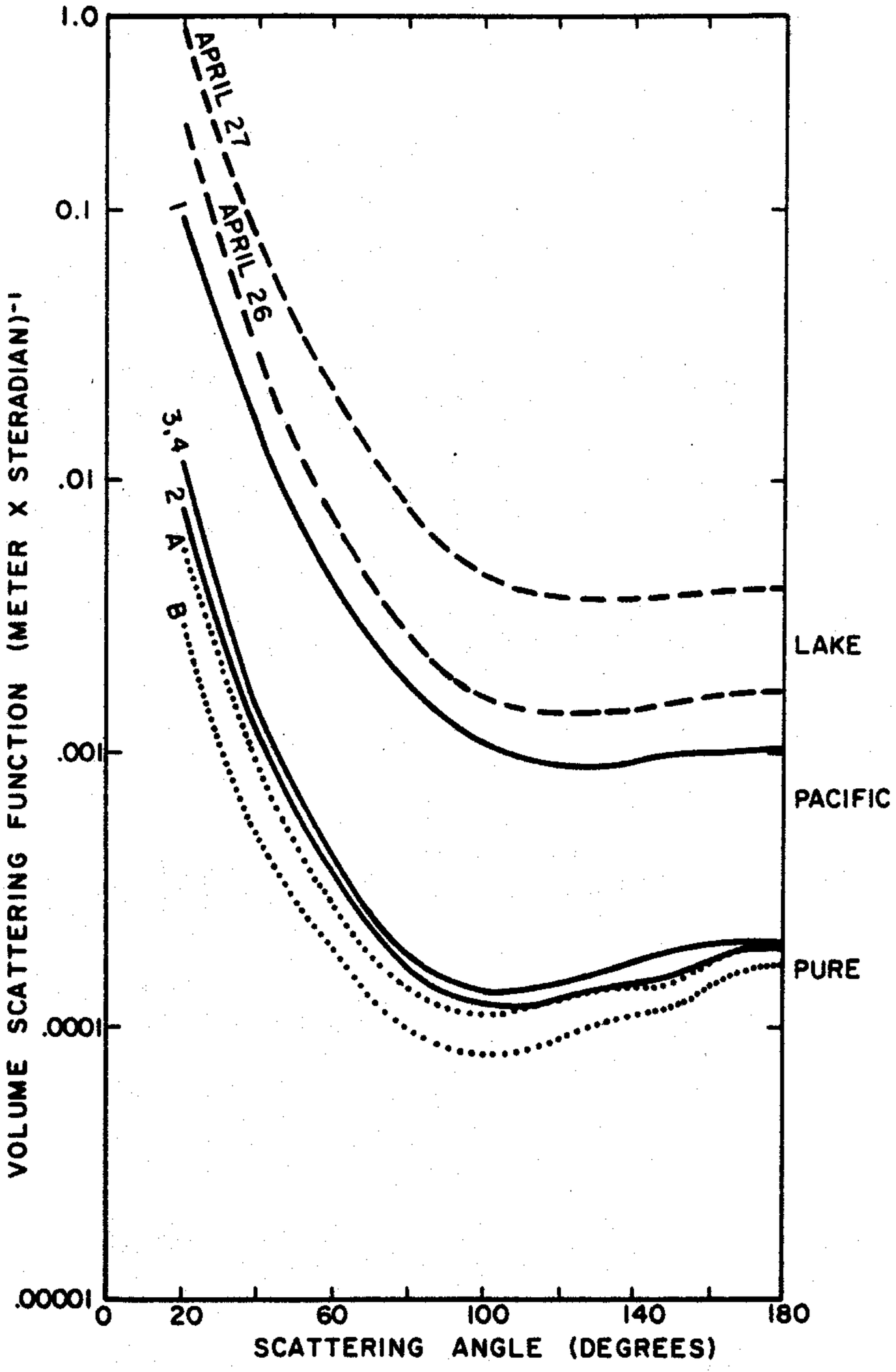


FIG. 1.70 Plot of Tables 1, 2, 3.

summarizes Tyler's Lake Pend Oreille measurements of the Spring of 1960. The wavelength band in this case was centered at 480 ± 64 mμ. These tabulations are compared graphically in Fig. 1.70 wherein the relative clarity of the waters may be seen at a glance. Curves 3, 4 of Table 2 essentially coincide in the figure.

Figure 1.71 provides three more comparisons of distilled, lake and ocean waters. In this case, the distilled water measurements were by Dawson and Hulburt [63], the lake water measurements by Duntley [78], and the Atlantic (between Madeira and Gibralter) measurements by Jerlov [123]. The latter graph is keyed in with the measurements listed in Table 4 below. The lake measurements by Duntley are of particular interest because of the relatively small angles for which σ was obtained using special equipment [78]. A detail of σ for the range 0.5° to 1.7° is given in Fig. 1.72. The ordinates of the lake curve in Fig. 1.71 are continued in Fig. 1.72.

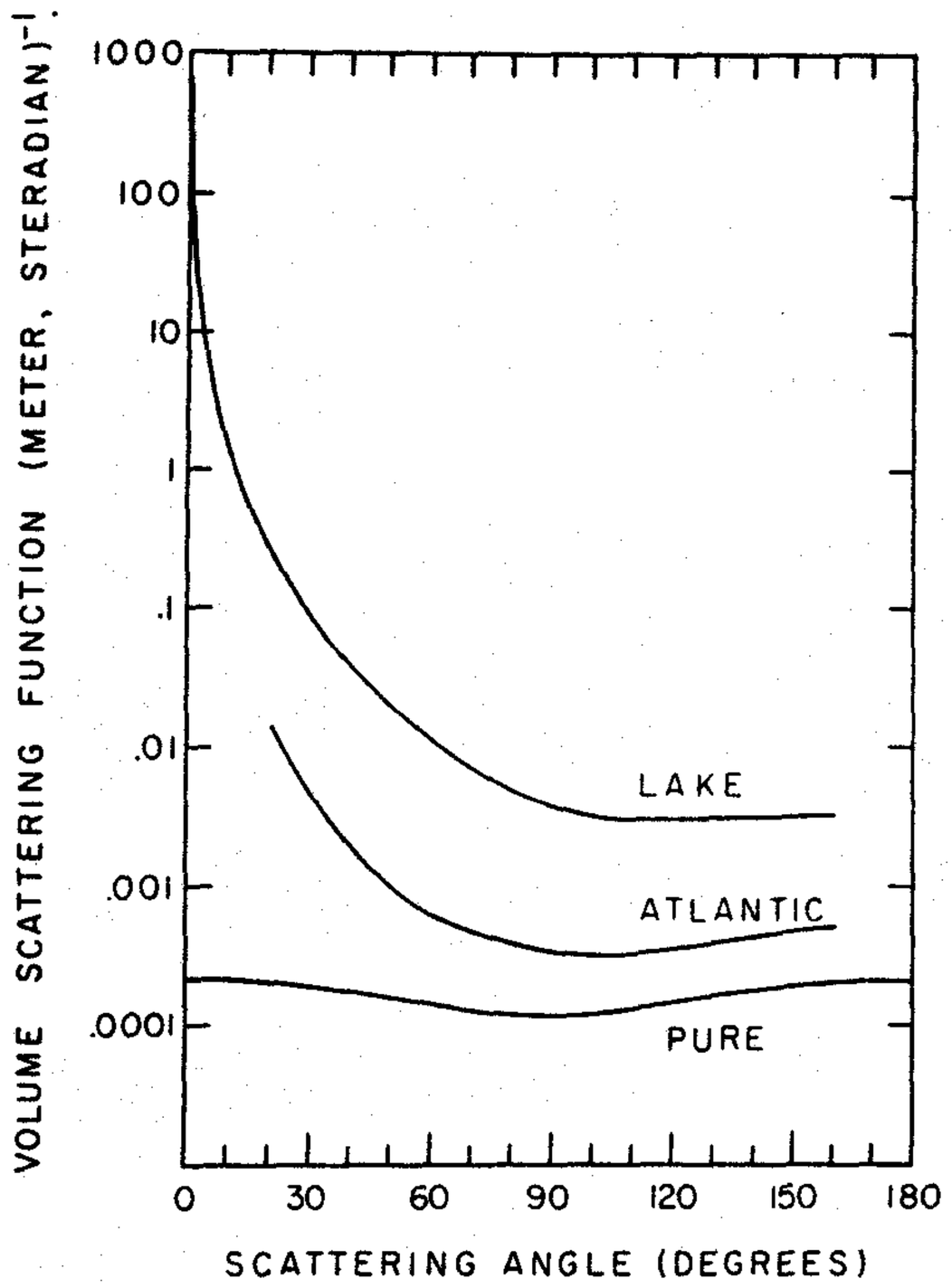


FIG. 1.71 Plots of data taken at various times and locales by Dawson and Hulburt (pure), by Duntley (lake), and by Jerlov (Atlantic). See text for details. (Fig. 9 from [78], by permission)

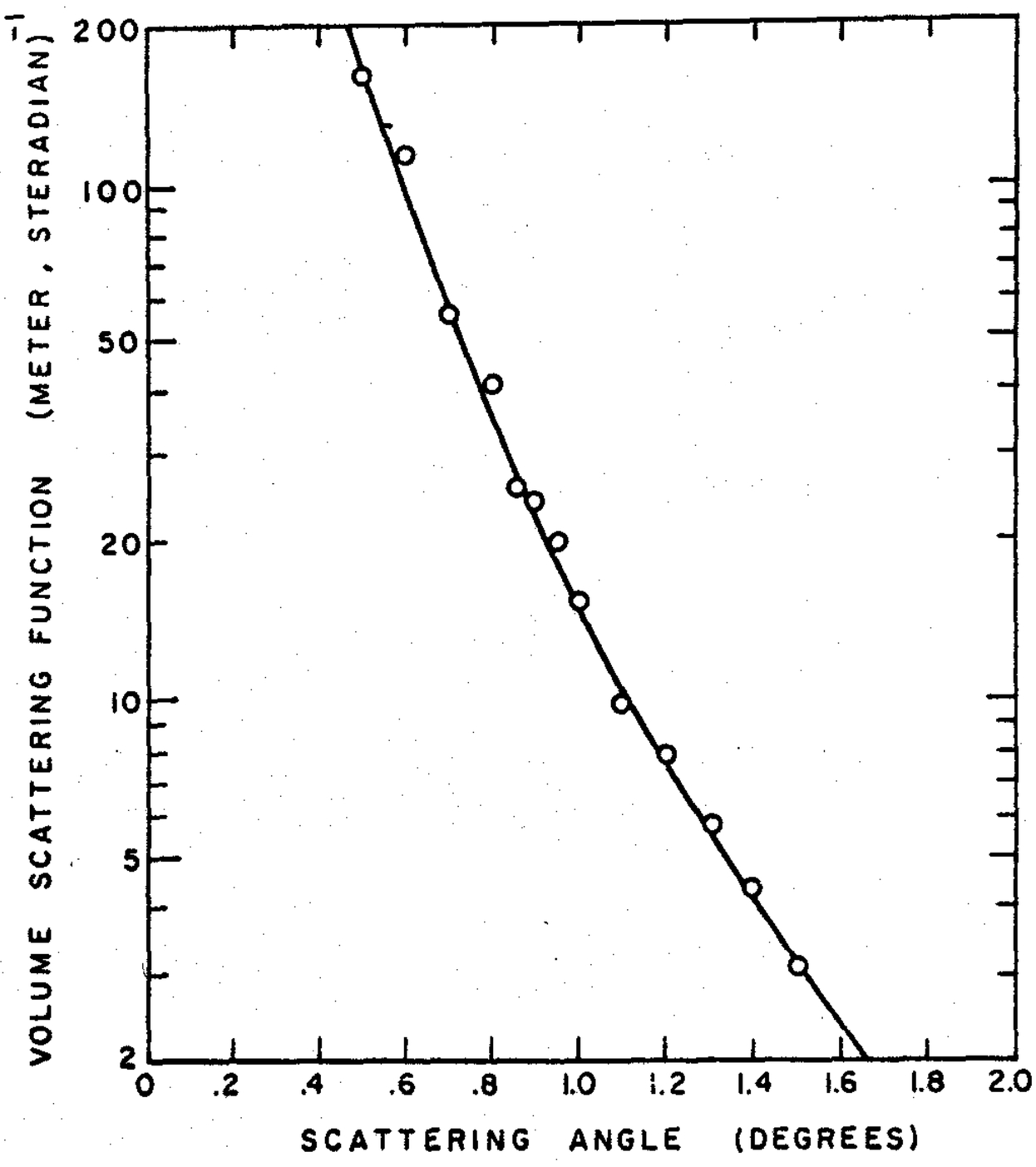


FIG. 1.72 Extreme detail of forward scattering values of volume scattering function in Duntley's lake water curve of Fig. 1.71.

TABLE 4

Comparison between relative values of the scattering function. (All data normalized at 90°)

| | In vitro measurements | | | In situ measurements | | |
|---|---|---|---|---|---|---|
| Angle θ | Poole and Atkins (1954) English Channel blue light | Hulburt (1945) Chesa-peake Bay white light | Kozlyan-inov (1957) East China Sea blue light | Sasaki (1960) Japan Trench 576 mμ | Jerlov (1961) East North Atlantic 465 mμ | Tyler (1961) Californian coast 522 mμ |
| 1° | | | 7200 | | | |
| 5° | | | 1100 | | (690) | |
| 10° | 232 | 247 | 312 | | 292 | |
| 20° | 62 | 61 | 62 | 39 | 74 | 67 |
| 30° | 18 | 22 | 22 | 22 | 23.5 | 20 |
| 45° | 6.0 | 8.5 | 6.9 | 5.5 | 7.5 | 6.7 |
| 60° | 2.5 | 3.0 | 3.1 | 2.9 | 2.96 | 2.70 |
| 75° | 1.5 | 1.4 | 1.8 | 1.2 | 1.72 | 1.51 |
| 90° | 1.0 | 1.0 | 1.0 | 1.0 | 1.00 | 1.00 |
| 105° | 0.82 | 1.0 | 0.49 | 0.8 | 0.95 | 0.91 |
| 120° | 0.67 | 1.2 | 0.44 | 0.7 | 1.05 | 0.94 |
| 135° | 0.90 | 1.5 | 0.50 | 1.0 | 1.30 | 1.05 |
| 150° | | 2.2 | | 1.2 | 1.55 | 1.18 |
| 165° | | 3.1 | | | 1.90 | 1.38 |
| 180° | | | | | (2.12) | 1.49 |

Errata

(From [127], by permission)

This shows how, in the space of 1°, near-forward scattering values soar two more orders of magnitude. The associated wavelengths are those transmitted by a No. 61 Wratten filter.

Further comparisons of σ values are made in Table 4 (patterned after [127]). Observe that Tyler's measurements are those listed for location 2 in Table 2. The main purpose of Table 4 is to show the remarkable similarity in shape of the σ curves, after normalization at 90°. This fact is reproduced graphically in Fig. 1.73. The curve labeled "Duntley (Green)" in Fig. 1.73 is the normalized lake curve of Fig. 1.71. The remaining references for the σ values of Table 4 and Fig. 1.73 are as follows: Atkins and Poole [6], Hulburt [115], Kozlyaninov [144], Sasaki et. al. [271], and Jerlov [123]. A relatively recent and somewhat extensive experimental study of σ in the Atlantic was made by Spilhaus [290]. This work makes new progress toward workable classifications of optical media via the volume scattering function.

The highly forward scattering character of natural waters observed in all of the preceding results is one of the

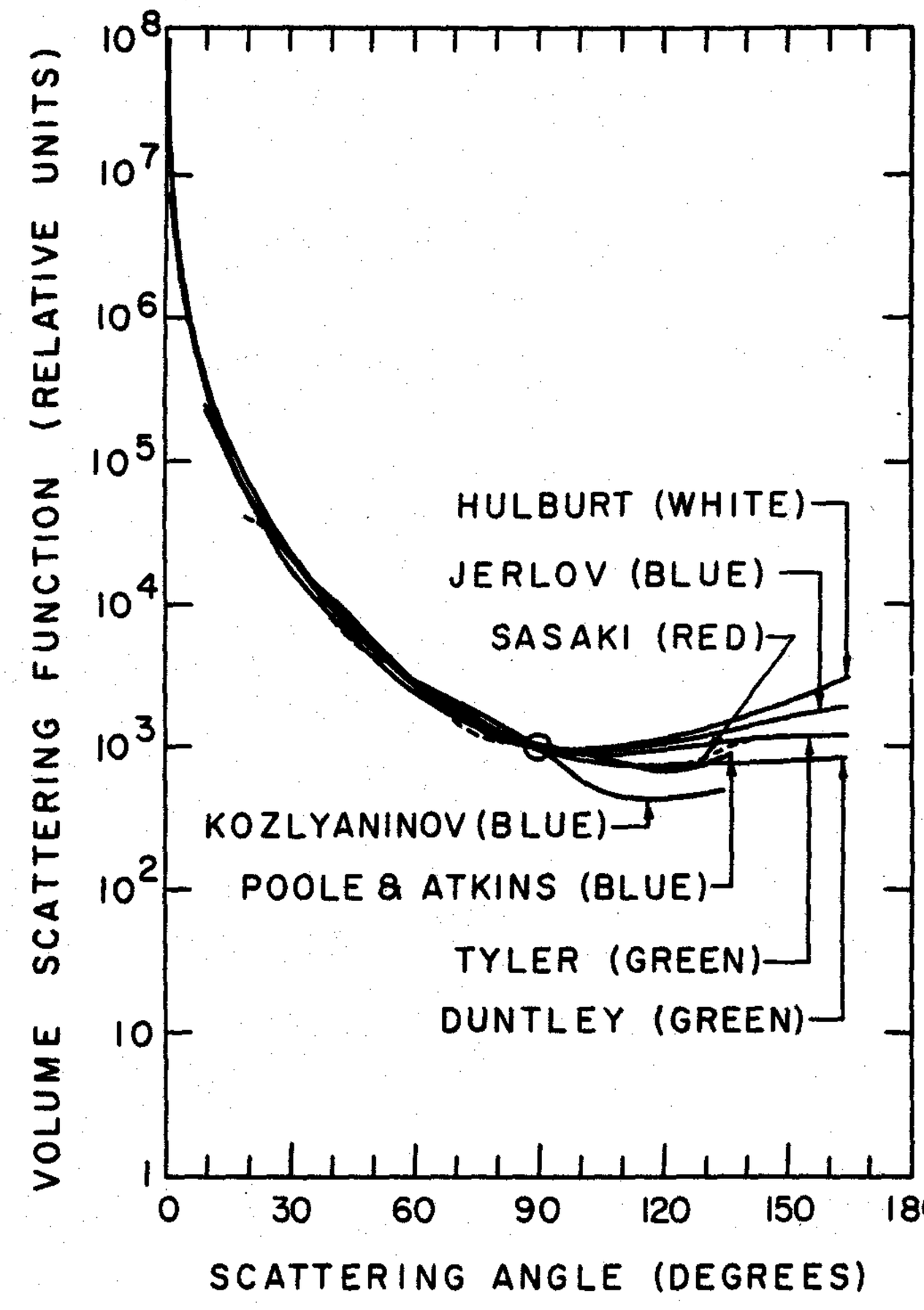


FIG. 1.73 Illustrating the stability of shape of the volume scattering function as measured in various locations and times. See text for details. (Fig. 12 from [78], by permission)

outstanding, and not yet fully understood features of the function. In particular, does the σ-curve have a vertical or horizontal tangent at 0°? Despite the absence of detailed knowledge, we know that the high forward scattering is due principally to the great variety of dissolved and suspended organic and mineral matter in the sea. The ebb and flow of the life processes and geologic processes within natural hydrosols constantly alters the concentration of these substances, and the basic Rayleigh-type scattering that absolutely pure water would exhibit is heavily masked by the scattered light produced by these 'foreign' substances. If water in its pristine state is examined optically, then (cf. [63]) the scattered radiance $N_r^*$ in (10) would have the general form:

$$N_r^*(\theta,\lambda) = \frac{Ar}{\lambda^4}(1 + B\cos^2\theta) \qquad (22)$$

where A and B are suitable constants (see [63]). Observe that $N_r^*(\theta,\lambda)$ increases sharply for the smaller wavelengths,

thereby tending to suffuse extensive masses of very pure water with scattered blue light, much in the way that the clear sunlit atmosphere above one's head appears blue to the sight. It was shown by Kalle [132] that the relatively heavy concentration of decaying organic matter in the form of phenol-humic acids and carbohydrate-humic acids (or melanoidines), respectively contribute the brownish and yellowish components to the otherwise clear blue water, the net result being the blue-green appearance of most natural hydrosols. Hence the greater the concentrations of these organic materials, the yellower or browner the water will become. Unlike the sharp $\lambda^{-4}$ wavelength-behavior of scattered light in pure water, we have, by contrast, in oceanic or lake water which contain particles and organisms whose dimensions are large compared with wavelengths of light, the scattered light nearly independent of wavelength. Hence when one measures $\alpha$ (= a+s) or k ($\cong \sqrt{aD(aD+2b)}$) as a function of wavelength and observes great variations, these variations are due principally to the absorption mechanism operative in the solutes and suspensoids within the water. For example, while the scattered light in pure water increases nearly 10 fold as $\lambda$ goes from 700 to 400 $m\mu$, the absorption coefficient for plankton-infested water or for suspensoids of the yellow substance increases on the order of 100 fold over the same range (cf., e.g., [115]). By virtue of these reasons, the striking similarity of shape of the $\sigma$ curves in Fig. 1.73 becomes more understandable. If this sensitivity of $\sigma$ to wavelength $\lambda$ is sufficiently weak, a great simplification of the documentation of optical properties of natural waters is possible; for then the burden of describing the spectral variation of the inherent optical properties falls on $\alpha$ or, equivalently, a. Table 5, adapted from Hulburt [115], gives the spectral dependence of $\alpha$, s, and a for two types of water. These tabulations bear out the rationalizations enunciated above. Table 6 shows the spread of $\alpha$ values over oceanic regions, as found by Jerlov [122].

TABLE 5

Spectral dependence of volume attenuation ($\alpha$), total scattering (s) and absorption functions (a) for distilled and Chesapeake Bay waters (per meter)

| Wavelength ($m\mu$) | Distilled | | | Bay | | |
|---|---|---|---|---|---|---|
| | $\alpha$ | s | a | $\alpha$ | s | a |
| 400 | .080 | .038 | .042 | - | - | - |
| 420 | .061 | .030 | .031 | .800 | .175 | .625 |
| 440 | .046 | .025 | .021 | .628 | .180 | .448 |
| 480 | .037 | .017 | .020 | .447 | .180 | .267 |
| 520 | .040 | .013 | .028 | .351 | .180 | .171 |
| 560 | .053 | .009 | .044 | .323 | .180 | .143 |
| 600 | .197 | .007 | .190 | .429 | .180 | .249 |
| 640 | .292 | .005 | .287 | .500 | .180 | .320 |
| 680 | .406 | .004 | .402 | .589 | .180 | .409 |
| 700 | .576 | .004 | .572 | .740 | .180 | .560 |

(From [115], by permission)

TABLE 6

Representative values of the volume attenuation function for various oceanic locations for 480 mμ wavelength.

| Location | α/meter | Attenuation length 1/α meters |
|---|---|---|
| Caribbean | .125 | 8 |
| Pacific N. Equatorial Current | .083 | 12 |
| Pacific counter current | .083 | 12 |
| Pacific Equatorial Divergence | .100 | 10 |
| Pacific S. Equatorial Current | .111 | 9 |
| Gulf of Panama | .167 | 6 |
| Galapagos Islands | .250 | 4 |

(From [122], by permission)

Before concluding this brief survey of the inherent optical properties of natural hydrosols we wish to point up an apparent dissimilarity between the spectral dependence of α in air and in water. The dissimilarity is with respect to the fine structure of the λ-dependence of α. In the meteorologic optics context, α experiences rather spectacular increases and decreases in values at frequent intervals along the λ-axis (see, e.g., Refs. [128], [296], and [177]). Where α decreases rapidly to some minimum at $\lambda_j$, the atmosphere is said to have a *window* at $\lambda_j$, for the beam tramsmittance $T_r = e^{-\alpha(\lambda)r}$ will have a *maximum* at $\lambda_j$, and so one can 'look through' the atmosphere with relative ease using light having wavelengths in the immediate neighborhood of $\lambda_j$. The infrared region of the spectrum, e.g., has windows through the atmosphere, and this fact has important consequences for communication applications of radiative transfer theory. These observations lead one to consider the possibility of a fine structure for α in natural waters. This possibility does not seem too bright, at least on the basis of Table 5. However, perhaps the measurements of α yielding the values in Table 5 were too crude, and accordingly smeared out possible sharp dips in α. That is, the minimum of α in the vicinity of 480 mμ for distilled water may harbor a still sharper minimum if the spectral resolution of α-meters were increased. Recently, a careful spectroscopic study of α for "battery-grade" distilled water was made in the region from 375 mμ to 685 mμ by Drummeter and Knestrick [68]. The spectral resolution achieved by the grating spectrograph used was .02 mμ. A path of water of 9.75 meters was used for the transmission experiment. Variations of α per meter as small as two parts in a hundred were capable of detection by the apparatus, i.e., the apparatus could detect changes Δα of $2 \times 10^{-2}$/m. No spectral fine structure of α of any significance was detectable.

## Operational Definitions of the Apparent Optical Properties

The *apparent optical properties* of a natural hydrosol are those radiometrically determined scattering- and absorbing-induced quantities which generally depend on the geometrical structure of the light field (i.e., whether the light field is more or less collimated or diffuse) but which have enough regular features and enough stability to be entitled to the appellation, "optical property". The main apparent optical properties are all measurable by means of the four irradiances: $h(z,\pm)$ and $H(z,\pm)$. (See (9), (10) of Sec. 1.1.) Thus we write:



| | | | | |
|---|---|---|---|---|
| "$D(z,\pm)$" | for | $\dfrac{h(z,\pm)}{H(z,\pm)}$ | (Distribution functions) | (23) |
| "$K(z,\pm)$" | for | $-\dfrac{1}{H(z,\pm)}\dfrac{dH(z,\pm)}{dz}$ | (K-functions for irradiance) | (24) |
| "$k(z)$" | for | $-\dfrac{1}{h(z)}\dfrac{dh(z)}{dz}$ | (K-function for scalar irradiance) | (25) |
| "$R(z,\pm)$" | for | $\dfrac{H(z,\mp)}{H(z,\pm)}$ | (Reflectance function for irradiance) | (26) |

The distribution functions are simple indicators of the collimatedness or diffuseness of the light field in the downward (-) or upward (+) flows. The three K-functions are the depth rates of decay of the various irradiances. They are in principle generally distinct, though numerically they are quite close in value. The R functions give the reflectance of the entire medium to upward (+) or downward (-) flux at level z. Each of these is implicitly a function of wavelength. The theory of their interconnections is quite simple and will be discussed briefly in the following section. Their full theory is established in Chapters 9, 10 and 13. Table 7, adapted from [306], is a representative sample of the magnitudes of these properties.

These measurements were made in the spring of 1957 before the onset of the plankton bloom and appearance of the thermocline. The lake was essentially homogeneous so that the values of $\alpha$, s, and a are representative of the entire medium. As the biologic activity within the lake increases throughout the remainder of the year, the values of $\alpha$, s and a will rise accordingly, thereby providing an optical biometer of such activity. Furthermore, since 95% of the radiant energy content of the lake is essentially confined to within 3 diffusion lengths 1/K of the surface (cf., (98) of Sec. 1.4) and is therefore within the arena of most biologic activity, we would expect the homogeneity of the lake to disappear with the onset of spring and summer. Furthermore, rain run-offs will introduce still further mixtures of organic and inorganic materials into the entire body of the lake and change the optical properties. In short, it appears quite possible for

TABLE 7

The apparent and inherent optical properties of Lake Pend Oreille at depth 29 meters and for a wavelength band centered on 480 ± 64 mμ

| Property | 28 April 1957 Computed from Radiance Dist. (sunny) | 16 March 1957 Measured Directly (overcast) | Calculated Indirectly |
|---|---|---|---|
| D(29,+) | 2.78 | | |
| D(29,-) | 1.31 | | |
| K(29,+) | .164/m | | |
| K(29,-) | .169/m | .184/m | |
| R(29,+) | 43.5 | | |
| R(29,-) | .023 | | |
| α(29) | | .442/m | |
| s(29) | | | .325/m |
| a(29) | .117/m | | |

(From [306], by permission)

one to form an optical portrait of the biology and geology of a lake or oceanic region by monitoring its α, σ, a and K, at given times over a yearly cycle. The more of these properties one records, the more complete will the optical portrait be, and the more likely will be the usefulness of the findings to scientists in neighboring disciplines to hydrologic optics.

In order to increase our intuitive and objective knowledge about the relations between the clarity of water and its α and K properties, we append Table 8, adapted from [74]. This table, while ostensibly a rather limited sample, exhibits some interesting relations between α and K. For example the list of values shows a remarkable stability of the ratio K/α considering the range of waters in which the measurements were made. Thus while α varies over an eightfold range and K over a sevenfold range, K/α varies only over about a twofold range. The stability of K/α within a given region of water is even greater, indicating a possible basis for simple rules of variation of α and K which may be used to estimate one of those properties in the absence of the other. This stability of K/α will be seen to be an important factor in the description of the shape of the light field at moderate and great depths in the seas and lakes (Sec. 10.7, in particular (29) of Sec. 10.7).

TABLE 8

A sampling of α, K values for the 480 ± 64 mμ range.

| | α | K | K/α |
|---|---|---|---|
| Coronados Islands, Mexico (depth: 3 to 10 meters) | 0.499 meter$^{-1}$ | 0.180 meter$^{-1}$ | .361 |
| San Diego Bay and Approaches (Average of data within 1/2 meter of the bottom) | | | |
| Open Sea Southwest of Point Loma | 0.439 meter$^{-1}$ | 0.177 meter$^{-1}$ | .404 |
| Coast at Mexico-California border | 0.654 | 0.226 | .346 |
| San Diego Harbor Opening | 0.727 | 0.162 | .223 |
| Zuniga Point, Harbor Opening | 1.065 | 0.396 | .372 |
| Entrance Channel, South | 1.156 | 0.280 | .242 |
| Entrance Channel, North | 1.770 | 0.565 | .320 |
| North Bend of Harbor | 1.462 | 0.584 | .400 |
| Midpoint of Harbor Pocket | 3.20 | 1.07 | .334 |
| Proceeding East through Straits of Juan de Fuca to Admiralty Inlet (Averages of data from 5 to 30 meters depth) | | | |
| Ocean Entrance | 0.543 meter$^{-1}$ | 0.262 meter$^{-1}$ | .483 |
| | 0.630 | 0.278 | .442 |
| Central Region | 0.600 | 0.315 | .525 |
| | 0.724 | 0.321 | .445 |
| Opposite Victoria, Vancouver Island | 0.651 | 0.340 | .522 |
| Fresh Water Lakes* | | | |
| El Capitan Reservoir (Aug. 1955), San Diego County (turbid water) | 1.853 meter$^{-1}$ | 1.062 meter$^{-1}$ | .575 |
| Diamond Island Field Station (Summer 1956) Lake Winnipesaukee, N.H. (moderately clear) | 0.756 | 0.374 | .495 |
| Lake Pend Oreille, Idaho (Apr 1957) (Clear water) | 0.413 | 0.195 | .472 |

*The coefficients α and K were found to be the same at all depths at these locations and times.

## Preliminary Observations on the Classification of Natural Hydrosols

From the preceding samplings, we see that one of the difficulties in forming a well-rounded optical picture of a natural hydrosol from most of the currently existing literature in hydrologic optics is that each investigator has looked at only one or two fragments of the entire radiometric picture according to his momentary interests. As a result, such findings have only transient interest because they cannot be incorporated by subsequent investigators into any systematic study of the radiative transfer processes occurring in the hydrosol. It is true that the preceding examples are very helpful in forming an intuition of the principal optical properties of natural hydrosols. However, the completeness of experimental studies to the degree shown in Tables 1, 2, 3 are all too rare and we can be hopeful that they will be emulated by other investigators in future scientific studies of light fields in oceans and lakes. The recent works of Tyler cited above and those of Jerlov [125], [126], [127], have begun to show a trend in the direction of exhaustive systematic optical analyses of natural hydrosols. Thus in Jerlov's work [127], potentially fruitful classifications of different types of ocean waters are made, and are elaborated in the book version of [125]. For example, Fig. 1.74 shows a classification of ocean water types by means of the irradiance

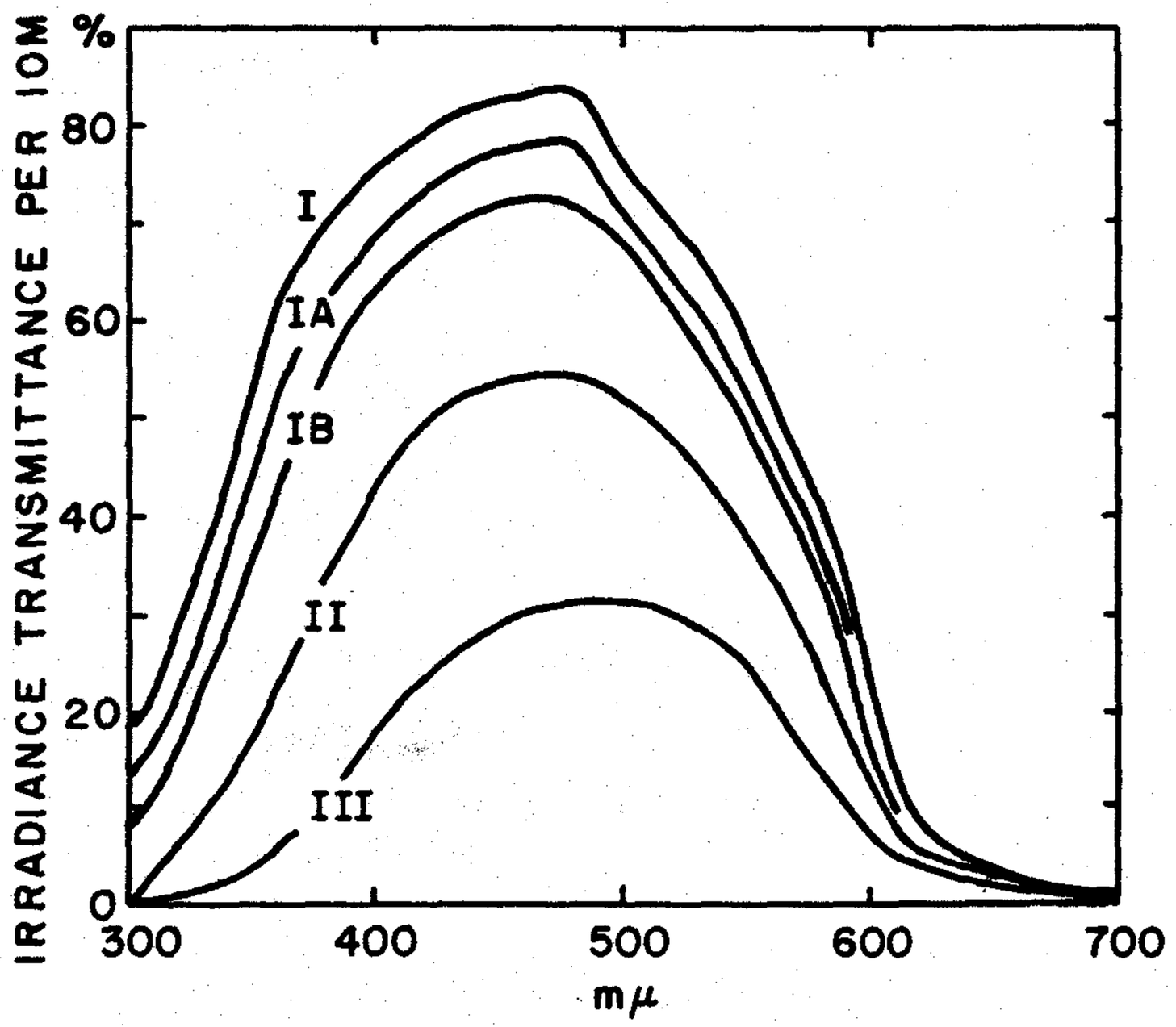


FIG. 1.74 Irradiance transmittance for a 10 meter layer of water, as sampled by Jerlov, and illustrating a possible classification scheme for natural hydrosols. (From [127], by permission)

transmittance $e^{-Kz}$ of a given layer of water ($z = 10$ meters in this case) as a function of wavelength. While it would be generally more desirable and more directly useful to simply plot the K-function for $H(z,-)$ as a function of $\lambda$, even as they stand, the graphs give an informative picture of the five general types of oceanic water encountered by Jerlov in his long series of careful studies of Atlantic and peripheral waters. These graphs could be of even greater service if someday they or their kind are supplemented by similar plots of $\alpha$ as a function of $\lambda$, along with $\sigma$, as a function of both $\theta$ and $\lambda$, if the patience and funds for such a pioneering effort could ever be assembled. The rationale behind these observations will be outlined in the following section.

<< Table of Contents << Title Page >> Next Page >>

## 1.7 Some General Modes of Classification of Natural Optical Media

Our studies in the preceding sections, especially those in the section just concluded, lead us to seek out those of the manifold optical properties used in the mathematical models of light fields in natural hydrosols that are fundamental and most useful. This problem has no simple solution, and indeed has different answers depending on one's view of the role of hydrologic optics in the study of natural waters. If one were a mathematician interested primarily in the intricate geometrical relations among the radiance distributions and their connections with the physics of the medium then, unquestionably, the inherent optical properties $\alpha$ and $\sigma$ as functions of position and wavelength (or equivalently $\alpha$ and a) constitute the only scientific answer to the query. If one were interested mainly in engineering calculations leading to estimates of the visibility of submerged objects in natural or artificial light fields then, equally clearly, the full spatial and spectral measurement of the properties $\alpha$ and K would suffice for most such purposes. On the other hand, a biologist interested in the problem of photosynthesis may find it possible to conduct a large portion of his work using only the volume absorption function a or only the diffuse attenuation function K. If one were a physicist or chemist concerned mainly with the analysis of water for the detection of certain dissolved and suspended substances, then quite likely $\sigma$ and $\alpha$ (or equivalently $\sigma$ and a) would suffice, but for vastly different reasons than those given by the mathematician mentioned above. For the mathematician would use $\alpha$ and $\sigma$ to compute $N(z,\xi)$ at each depth z and for each direction $\xi$, while the physicist or chemist would use $\alpha$ and $\sigma$ to yield concentrations of solutes and suspensoids in the irradiated sample of the hydrosol.

### Modes of Classification

In view of the preceding observations, several alternate modes of classification of natural optical media are possible. We now list the main modes of classification and indicate how much information about the hydrosol is inherent in each.